Supplement of Atmos. Chem. Phys. Discuss., 14, 20259–20293, 2014
http://www.atmos-chem-phys-discuss.net/14/20259/2014/
doi:10.5194/acpd-14-20259-2014-supplement

Atmospheric Chemistry and Physics Discussions

Supplement of

Seasonal characteristics of fine particulate matter (PM) based on high resolution time-of-flight aerosol mass spectrometric (HR-ToF-AMS) measurements at the HKUST Supersite in Hong Kong

Y. J. Li et al.

Correspondence to: C. K. Chan (keckchan@ust.hk)

1. Site location

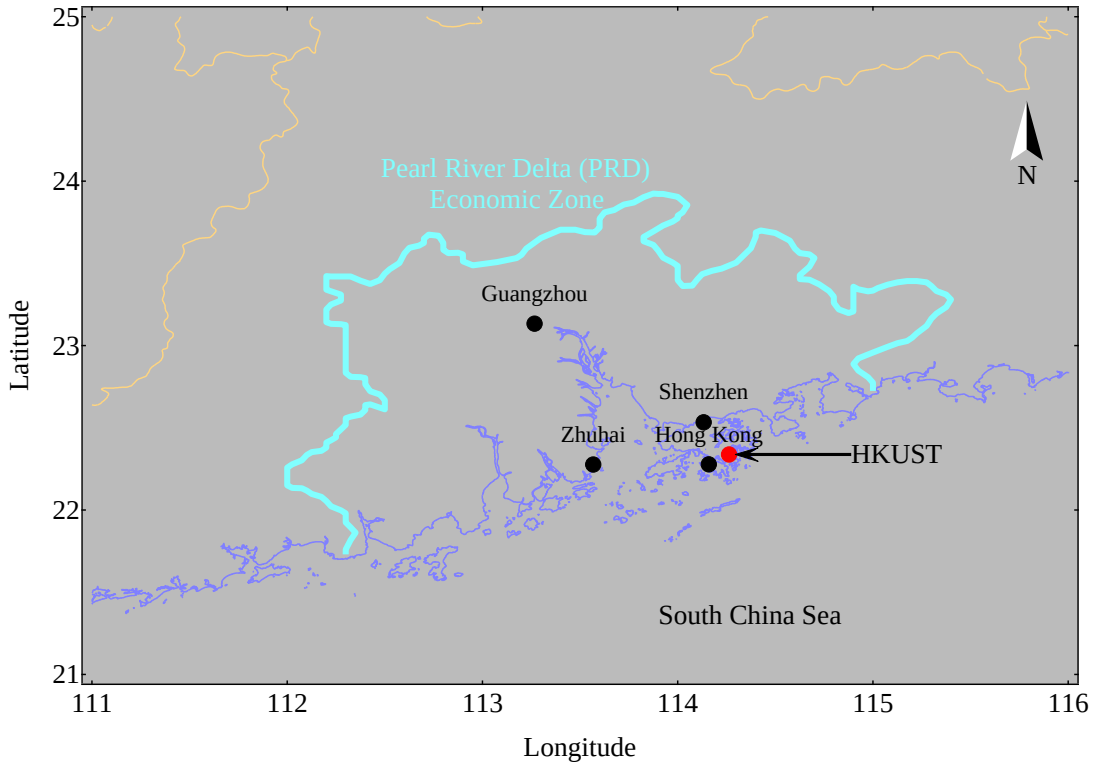

Figure S1 Location of the sampling site in the Pearl River Delta (PRD) region

2. Aerosol mass spectrometer (AMS) measurement

In pToF mode, the instrument performs particle sizing based on particle time-of-flight with the aid of a chopper and gives size-resolved chemical composition data in vacuum aerodynamic diameter (D_{va}) (DeCarlo et al., 2004). In V mode, the shorter traveling path for ions in the ion time-of-flight (iToF) chamber gives a mass spectral resolving power of approximately 2000 and better sensitivity. In W mode, the mass spectral resolving power is approximately 4000 but the signal-to-noise ratio is lower. The instrument was operated alternately between the V+pToF combined mode and the W mode for 5 minutes each. The sampling inlet was shared by a few instruments and an extra pump was used to maintain the required flow rate (16.7 L/min) for the $PM_{2.5}$ size cut. A diffusion dryer (BMI, San

Francisco, CA) was placed before the inlet of the HR-ToF-AMS to remove particulate water.

Ionization efficiency (IE) calibrations were performed weekly using size-selected ammonium nitrate particles (350 nm in mobility diameter, Dm). The flow rate of the inlet (~80 ml/min) and sizing (using standard PSL particles, Duke Scientific, Palo Alto, CA) were calibrated before and after the campaigns and negligible differences were observed. Frequent filtered periods (normally daily, maximum in three days) by putting an HEPA filter in front of the instrument inlet were performed for 30 to 60 min (3 to 6 data points for each mode). The results from the filter periods serve two purposes. First, the measured concentrations of all species in the "background" air can be used to calculate the campaign detection limits (CDLs) (Figures S2 and S3). Second, the intensities of ions affected by gaseous species (e.g., m/z 15, 16, 29, and 44) in the filter periods can be used to obtain more representative coefficients in the fragmentation table, which are essential for assigning signal intensities to particulate species. The correction factors (in addition to the original coefficients in the default fragmentation table) are given in Table S1 for all four months. In addition, the contribution of gaseous CO_2 to the variation in m/z 44 was corrected from the time-series of gaseous CO_2 concentrations (an additional season-dependent dynamic CO2_factor in Table S1) according to previous studies (Setyan et al., 2012;Collier and Zhang, 2013).

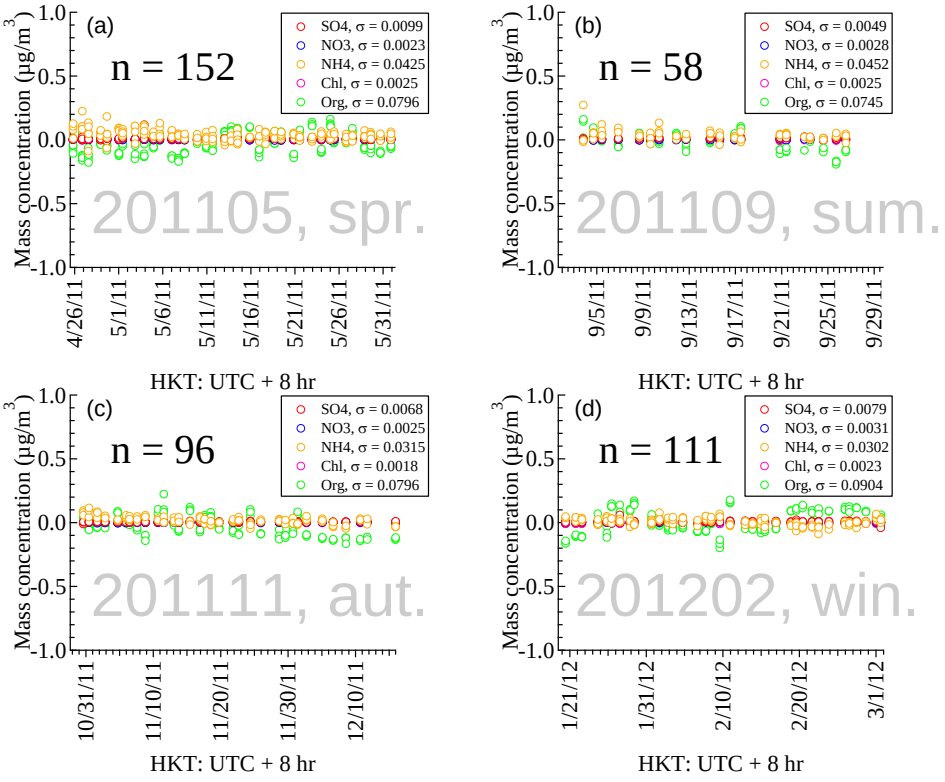

Figure S2 Mass concentrations of sulfate (SO4), nitrate (NO3), ammonium (NH4), chloride (Chl), and organics (Org) in the daily filter periods. In 201105, one-hour filter periods were performed daily while in other months 30 min filter periods were performed.

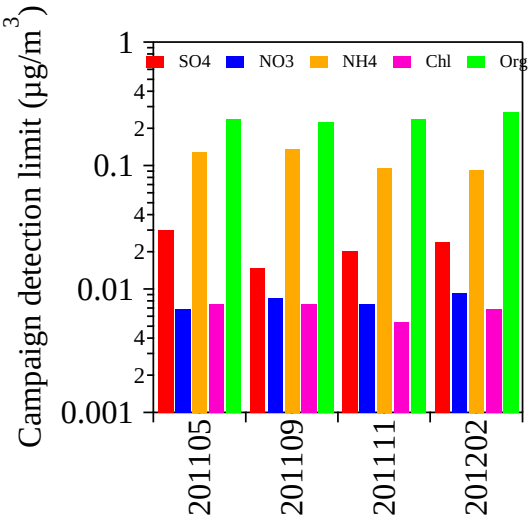

Figure S3 Four-month campaign detection limits (CDLs) of all five species as estimated by 3 times standard deviations of the concentration measured in filter periods.

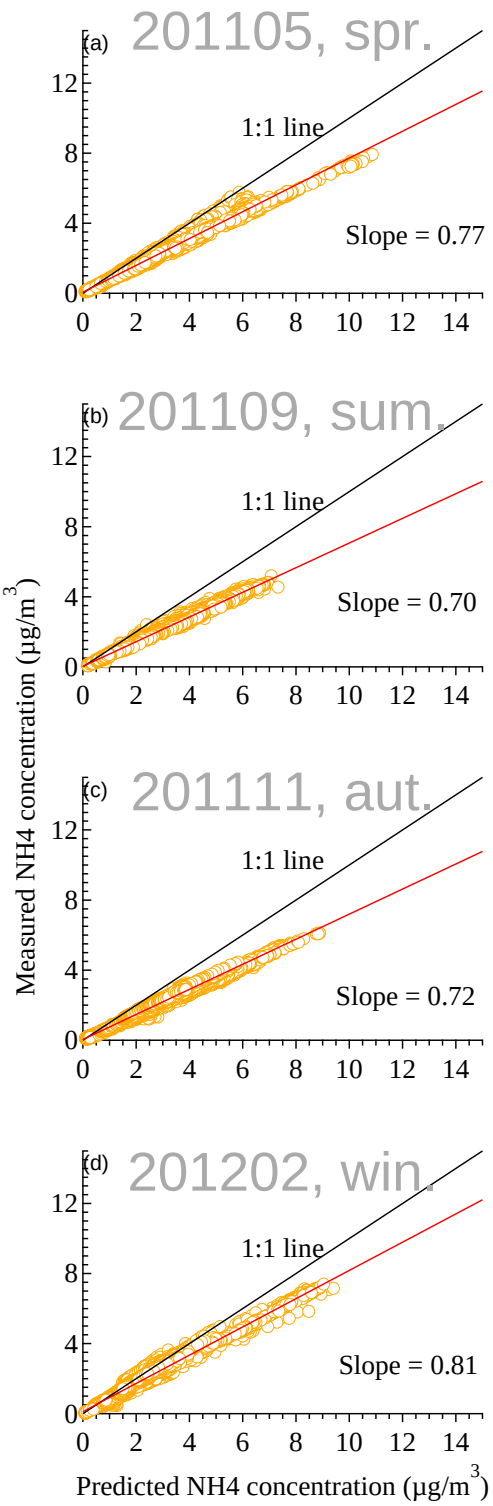

Figure S4 Measured vs predicted ammonium concentration in four seasons. Predicted ammonium concentrations are calculated by $NH_{4,p} = 18 \times (2 \times SO_{4,\,m}/96 + NO_{3,m}/62 + Chl_m/35.5)$, where "p" denotes "predicted" and "m" denotes "measured".

3. Modification to fragmentation table

Table S1 Coefficients used to correct the ion contribution to organic signals in addition to those used in the default fragmentation table.

	m/z 15	m/z 16	m/z 29	m/z 44
201105, spring	0.87	1.06	0.80	0.90 × CO_2_factor
201109, summer	0.90	1.11	0.77	0.85 × CO_2_factor
201111, autumn	0.85	1.04	0.72	0.80 × CO_2_factor
201202, winter	0.79	1.04	0.64	0.70 × CO_2_factor

4. Non-refractory PM_1 measured by AMS in Asia

Table S2 Summary of AMS measurements in Asia.

Location	Acronym[a]	Sampling period	Characteristic	Inorganics			Organics		Elemental analysis		Reference	AMS[f]
				Sulfate	Nitrate	Ammonium	POA[b]	OOA[c]	O:C[d]	H:C[e]		
Eastern Asia	–	Apr., 2001	ground	6.08 ± 1.80	2.31 ± 1.45	2.03 ± 1.30	7.13 ± 3.88		–	–	(Bahreini et al., 2003)	(1)
			< 100 m	3.01 ± 2.08	0.97 ± 0.75	1.32 ± 0.34	4.46 ± 2.70		–	–		
			100 - 1000 m	2.49 ± 1.74	1.13 ± 0.54	1.06 ± 0.48	6.06 ± 3.78		–	–		
			1000 - 3000 m	2.34 ± 2.61	0.55 ± 0.50	1.58 ± 1.20	3.65 ± 2.47		–	–		
			> 3000 m	1.41 ± 1.11	0.41	3.38	2.62 ± 2.36		–	–		
Jeju Island, Korea	JJK	Apr., 2001	remote	3.09 ± 1.74	0.51 ± 0.55	1.48 ± 1.45	3.49 ± 3.14		–	–	(Topping et al., 2004)	(1)
Fukue, Japan	FKJ	Mar. and Apr., 2003	remote	4.80	0.56	1.57	5.03		–	–	(Takami et al., 2005)	(1)
Tokyo, Japan	TKJ	Feb., 2003	urban	$2.5^{3.6}_{1.5}$	$3.1^{8.7}_{0.8}$	$2.2^{4.7}_{1.1}$	$6.7^{10.5}_{3.4}$		–	–	(Takegawa et al., 2006)	(1)
		Jul. – Aug., 2003		$3.2^{4.7}_{2.0}$	$1.0^{2.3}_{0.4}$	$1.8^{2.7}_{1.0}$	$5.7^{8.9}_{3.5}$		–	–		
		Sep. – Oct., 2003		$1.8^{2.6}_{1.1}$	$1.0^{2.9}_{0.5}$	$1.3^{2.0}_{0.7}$	$7.1^{10.3}_{4.6}$		–	–		
		Jan. – Feb., 2004		$1.7^{2.5}_{1.2}$	$2.8^{5.6}_{1.3}$	$2.3^{3.9}_{1.4}$	$5.8^{9.4}_{3.7}$		–	–		
Okinawa, Japan		Mar., 2005	remote	6.37 ± 4.30	–	1.25 ± 0.94	2.16 ± 1.60		–	–	(Takami et al., 2007)	(1)
Qingyuan, China	QYC	Jul., 2006	rural/SE-south	13.4 ± 8.6	1.3 ± 1.4	4.1 ± 2.7	12.8 ± 7.8		–	–	(Xiao et al., 2011)	(1)
			rural/southwest	10.1 ± 3.8	1.0 ± 0.5	3.3 ± 1.5	15.7 ± 6.3		–	–		
			rural/north	14.8 ± 9.6	1.8 ± 2.0	5.2 ± 3.9	18.7 ± 10.9		–	–		
			rural/east	4.7 ± 3.7	1.4 ± 1.8	2.0 ± 1.8	7.3 ± 5.3		–	–		
Beijing, China	BJC	Jul., 2006	urban	20.3 ± 11.6	17.3 ± 13.2	13.1 ± 7.4	11.0	17.1	–	–	(Sun et al., 2010)	(1)
Yufa, China	YFC	Aug. – Sep., 2006	suburban	8.20 ± 7.46	2.88 ± 2.51	4.07 ± 3.23	10.83 ± 7.79		–	–	(Gunthe et al., 2011)	(1)
Beijing, China	BJC	Jul. – Sep., 2008	urban	16.8	10.0	10.0	10.2	13.7	–	–	(Huang et al., 2010)	(3)
Kaiping, China	KPC	Oct. – Nov., 2008	rural	11.1	3.5	4.6	2.7	8.5	0.47 ± 0.07	1.48 ± 0.08	(Huang et al., 2011)	(3)
Shenzhen, China	SZC	Oct. – Dec., 2009	urban	10.9	4.5	4.5	8.2	9.5	0.30 ± 0.06	1.63	(He et al., 2011)	(3)
Shanghai, China	SHC	May – Jun., 2010	urban	9.7	4.8	3.9	2.0	6.4	0.31	1.64	(Huang et al., 2012)	(3)
Jiaxing, China	JXC	Jun. – Jul., 2010	suburban	8.3	5.9	4.1	3.3	7.2	–	–	(Huang et al., 2013)	(3)
		Dec., 2010		7.1	7.5	4.9	5.0	7.7	–	–		
Tianjin, China	TJC	Sep., 2010	urban	14.4	16.2	13.6	15.7		–	–	(Zhang et al., 2012)	(2)
Wakayama, Japan	–	Aug., 2010	forest	1.6	–	0.5	1.8		–	–	(Han et al., 2014)	(3)
Heshan, China	HSC	Nov., 2010	urban outflow	10.0	6.2	4.6	5.6	11.8	0.40 ± 0.06	1.49 ± 0.07	(Gong et al., 2012)	(3)
Changdao, China	CDC	Mar. – Apr., 2011	receptor	8.3 ± 7.3	12.2 ± 12.0	6.5 ± 6.0	4.4	9.4	0.59 ± 0.10	1.33 ± 0.07	(Hu et al., 2013)	(3)
Beijing, China	BJC	Jun. – Aug., 2011	urban	9.0	12.4	8.0	7.1	12.7	–	–	(Sun et al., 2012)	(4)
Gwangju, Korea	GJK	Sep., 2011	urban	1.75 ± 0.85	0.62 ± 0.27	1.07 ± 0.63	4.70 ± 1.81		–	–	(Park et al., 2012)	(1)
		Dec., 2011		1.90 ± 0.57	2.45 ± 1.03	1.70 ± 0.67	6.31 ± 1.77		–	–		
Beijing, China	BJC	Nov., 2011 – Jan., 2012	urban	9.3	10.9	8.6	23.7	10.7	–	–	(Sun et al., 2013)	(4)
Beijing, China	BJC	Jan., 2013 (unpolluted)	urban	3.5	1.4	1.4	5.9	3.2	0.34 ± 0.08	1.44 ± 0.05	(Zhang et al., 2014)	(3)
		Jan., 2013 (polluted)		39.2	22.4	15.4	21.2	36.2				
Hong Kong, China	HKC	May, 2011	suburban	7.4 ± 4.5	0.6 ± 0.7	2.3 ± 1.4	0.8	3.2	0.38 ± 0.11	1.35 ± 0.11	This study	(3)
		Sep., 2011		8.7 ± 3.8	0.4 ± 0.4	2.4 ± 1.0	0.7	3.4	0.52 ± 0.12	1.36 ± 0.11		
		Nov., 2011		7.1 ± 3.7	0.7 ± 0.5	2.1 ± 1.1	0.8	5.2	0.42 ± 0.08	1.39 ± 0.07		
		Feb., 2012		6.2 ± 3.2	1.6 ± 1.4	2.4 ± 1.2	1.0	4.1	0.43 ± 0.07	1.40 ± 0.06		

[a]: Acronyms of the sampling locations used in Figure 2. [b]: Primary organic aerosols (POA) include one or more of hydrocarbon-like organic aerosols (HOA), cooking organic aerosols (COA), biomass burning organic aerosols (BBOA), and coal-combustion organic aerosols (CCOA); [c]: Oxygenated organic aerosols (OOA) include either OOA I and OOA II or low-volatility oxygenated organic aerosols (LVOOA) and semi-volatile oxygenated organic aerosols (SVOOA); [d]: oxygen-to-carbon atomic ratio (O:C); [e]: hydrogen-to-carbon atomic ratio (H:C); [f]: Type of AMS, (1) is Quadrople AMS (Q-AMS), (2) is compact Time-of-Flight AMS (c-ToF-AMS), (3) is High-Resolution Time-of-Flight AMS (HR-ToF-AMS), (4) is Aerosol Chemical Speciation Monitor (ACSM).

5. PMF diagnostics and evaluation

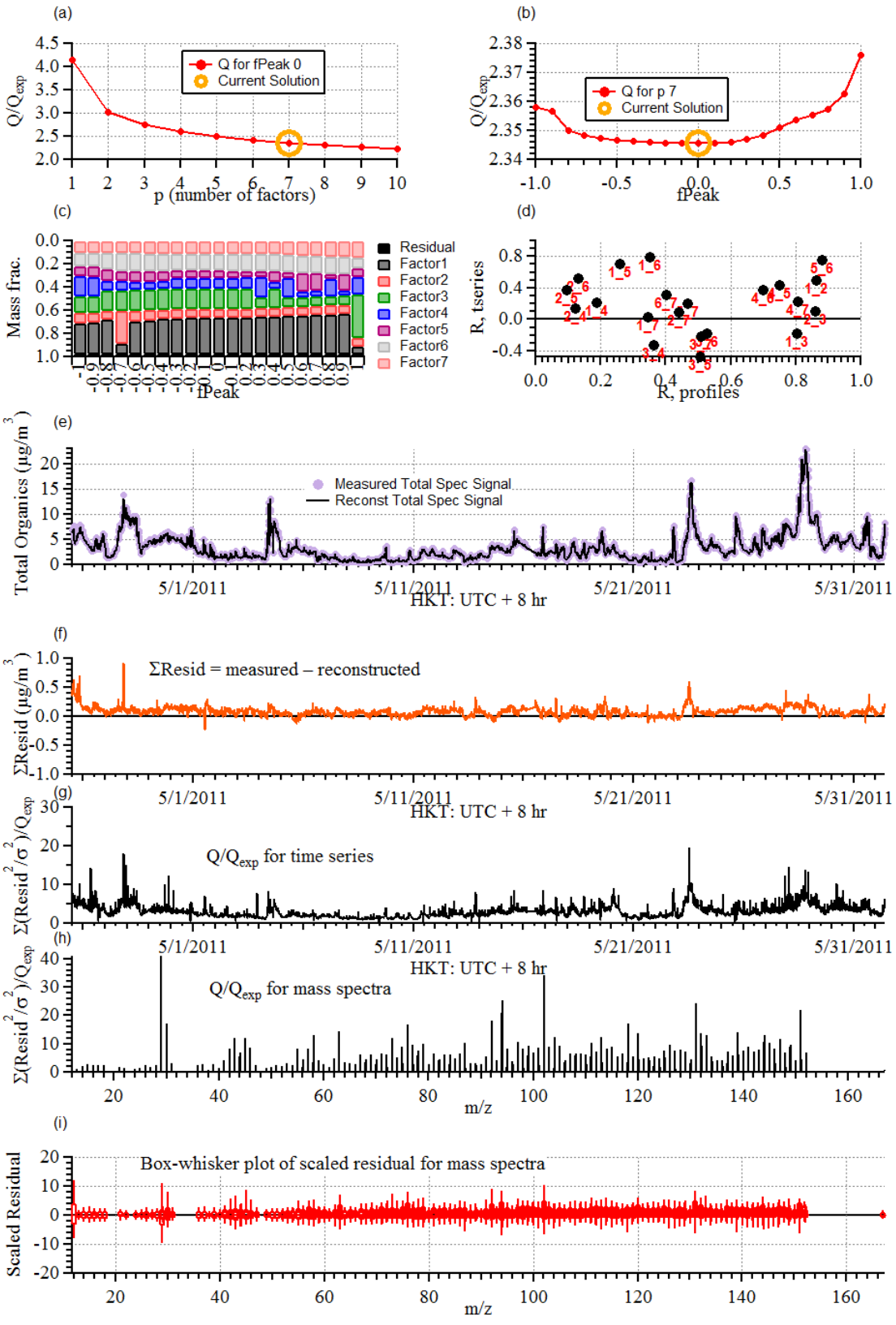

Figure S5 Diagnostic plot for 201105, spring.

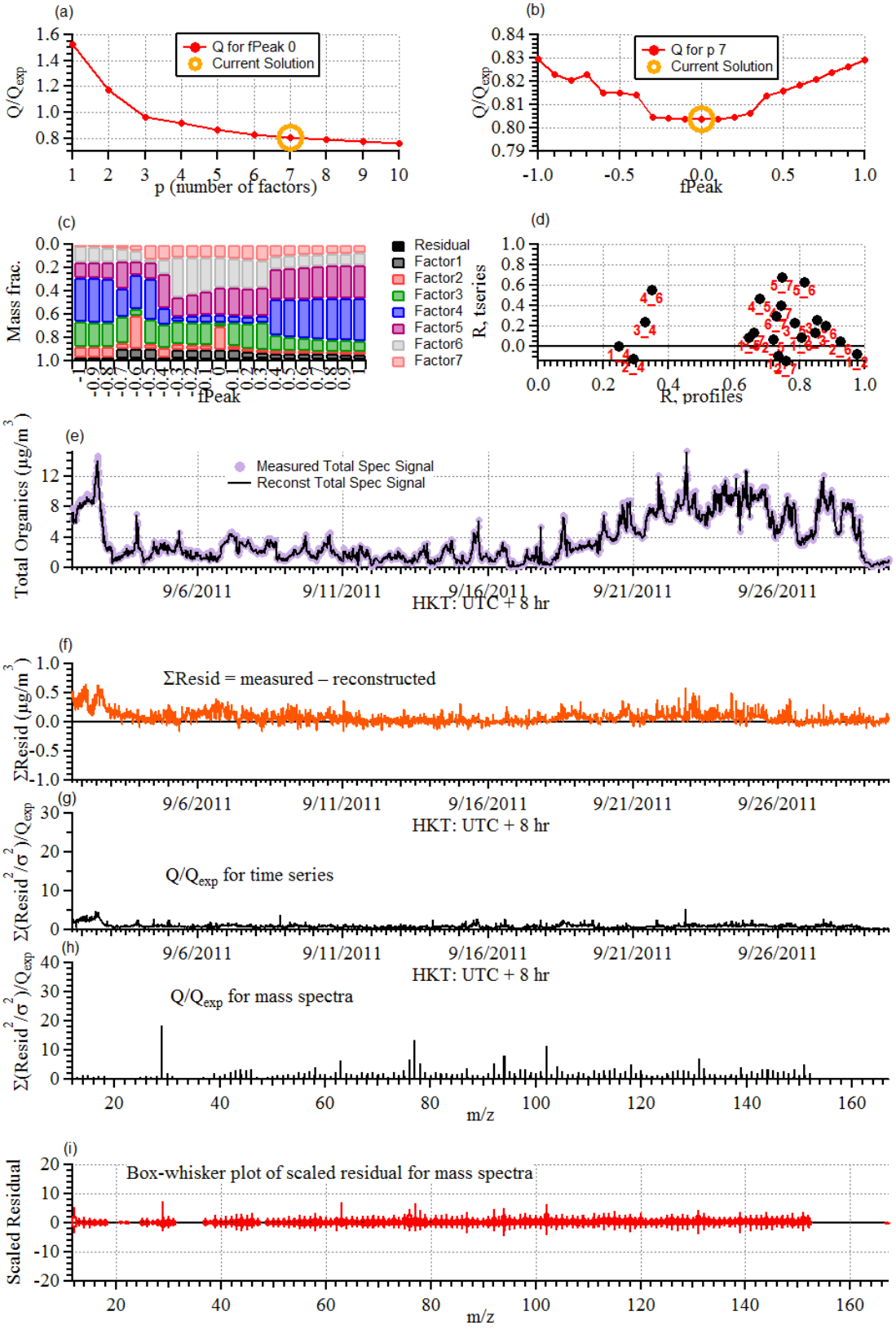

Figure S7 Diagnostic plot for 201109, summer.

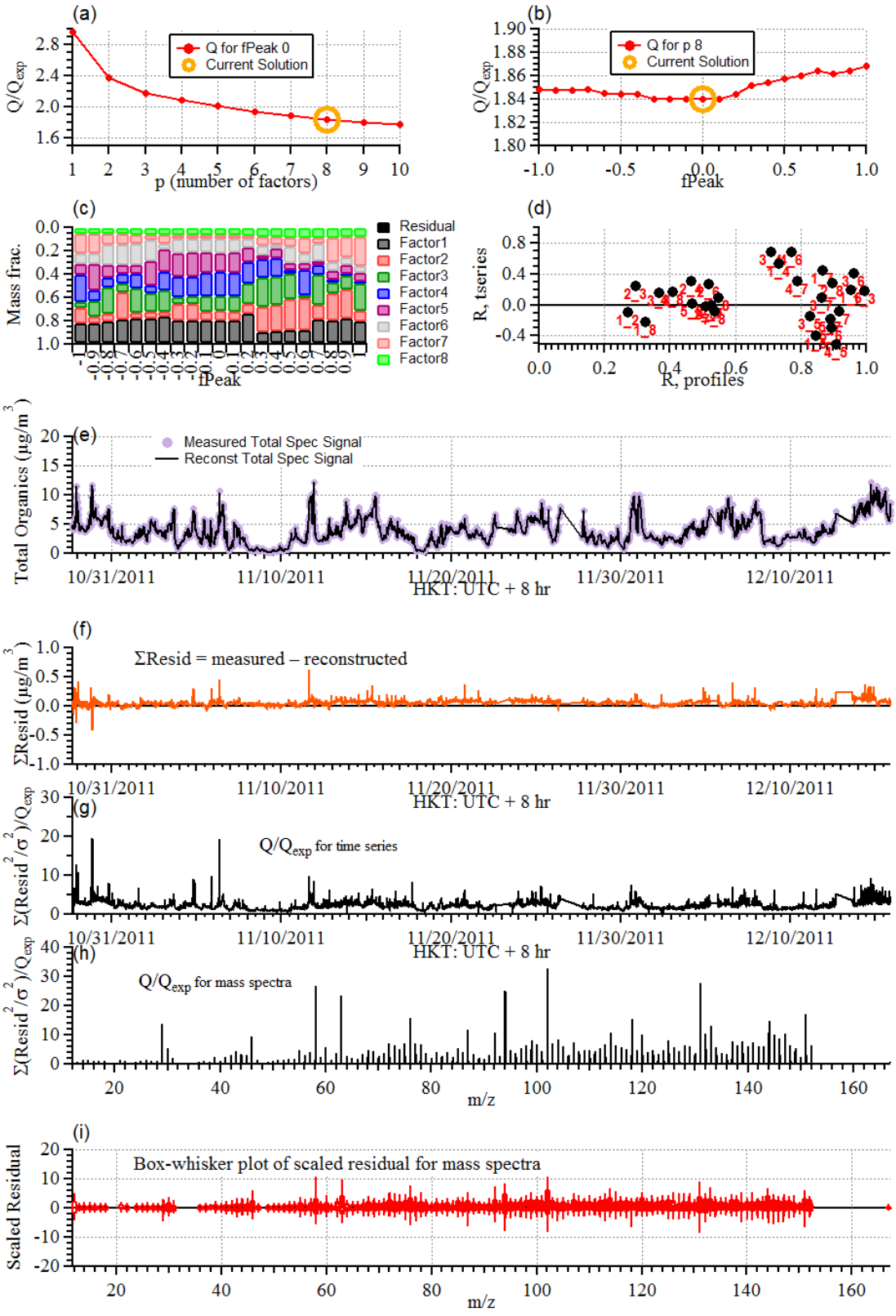

Figure S7 Diagnostic plot for 201111, autumn.

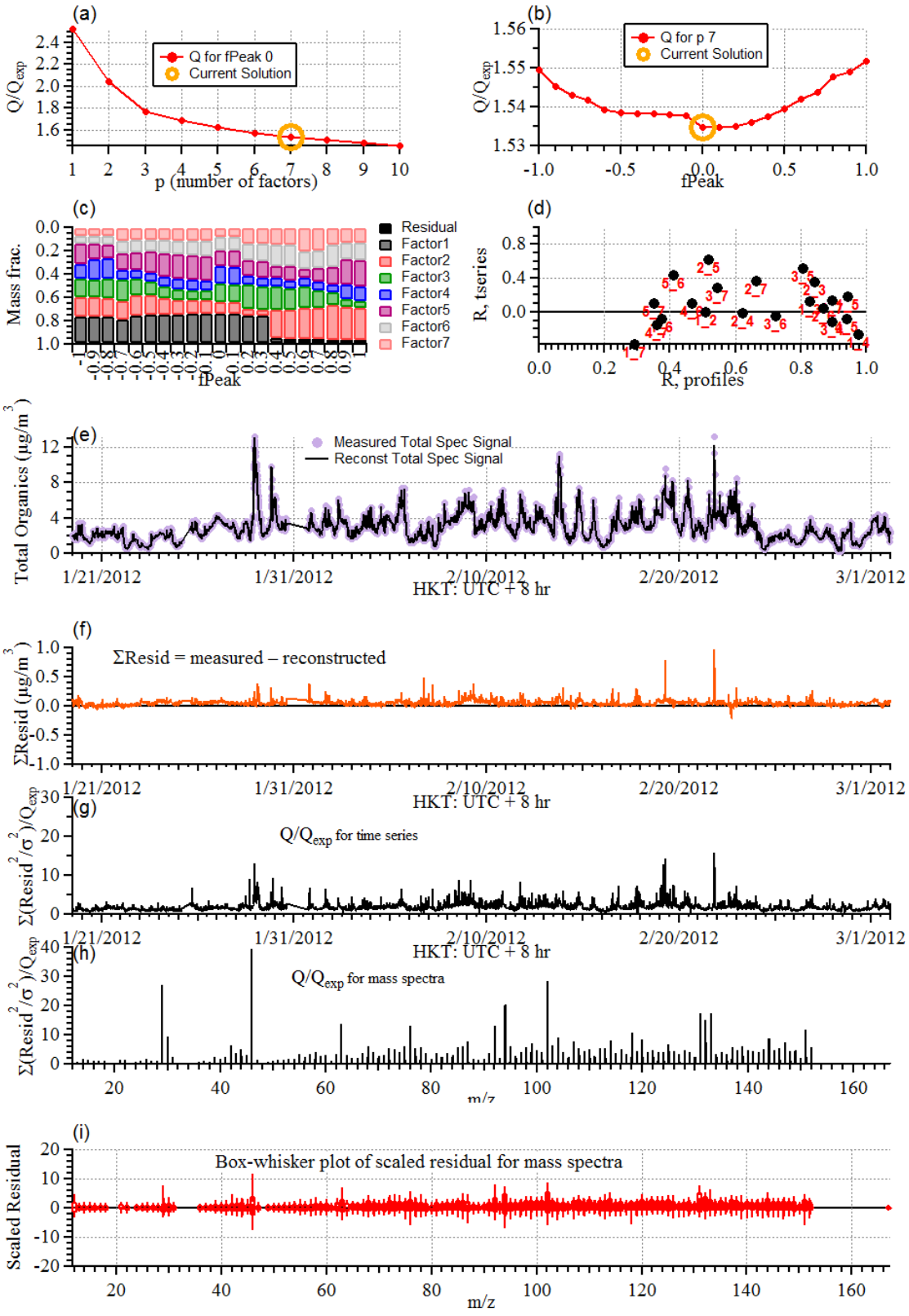

Figure S8 Diagnostic plot for 201202, winter.

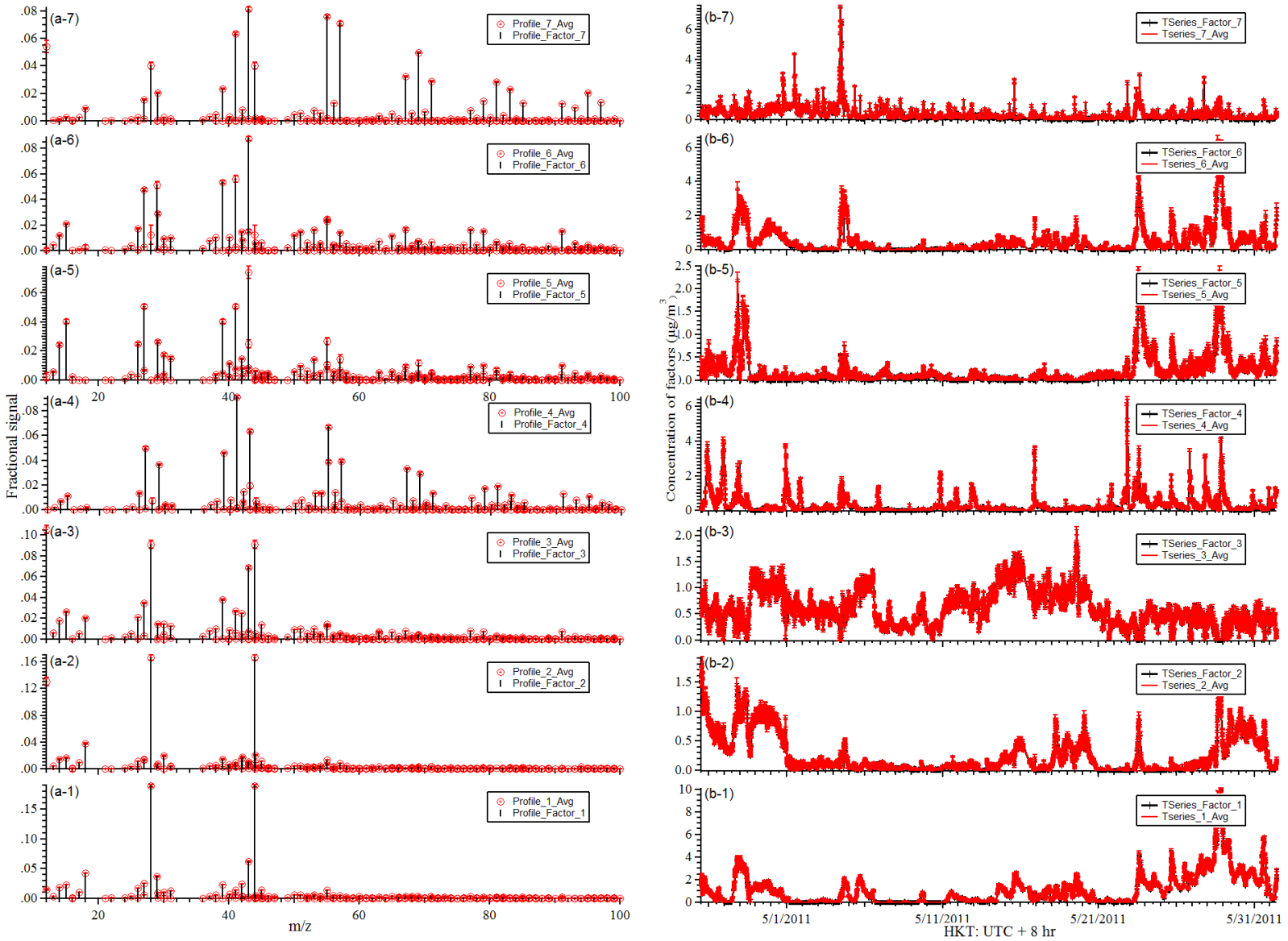

Figure S9 Example of bootstrapping plot (201105, spring).

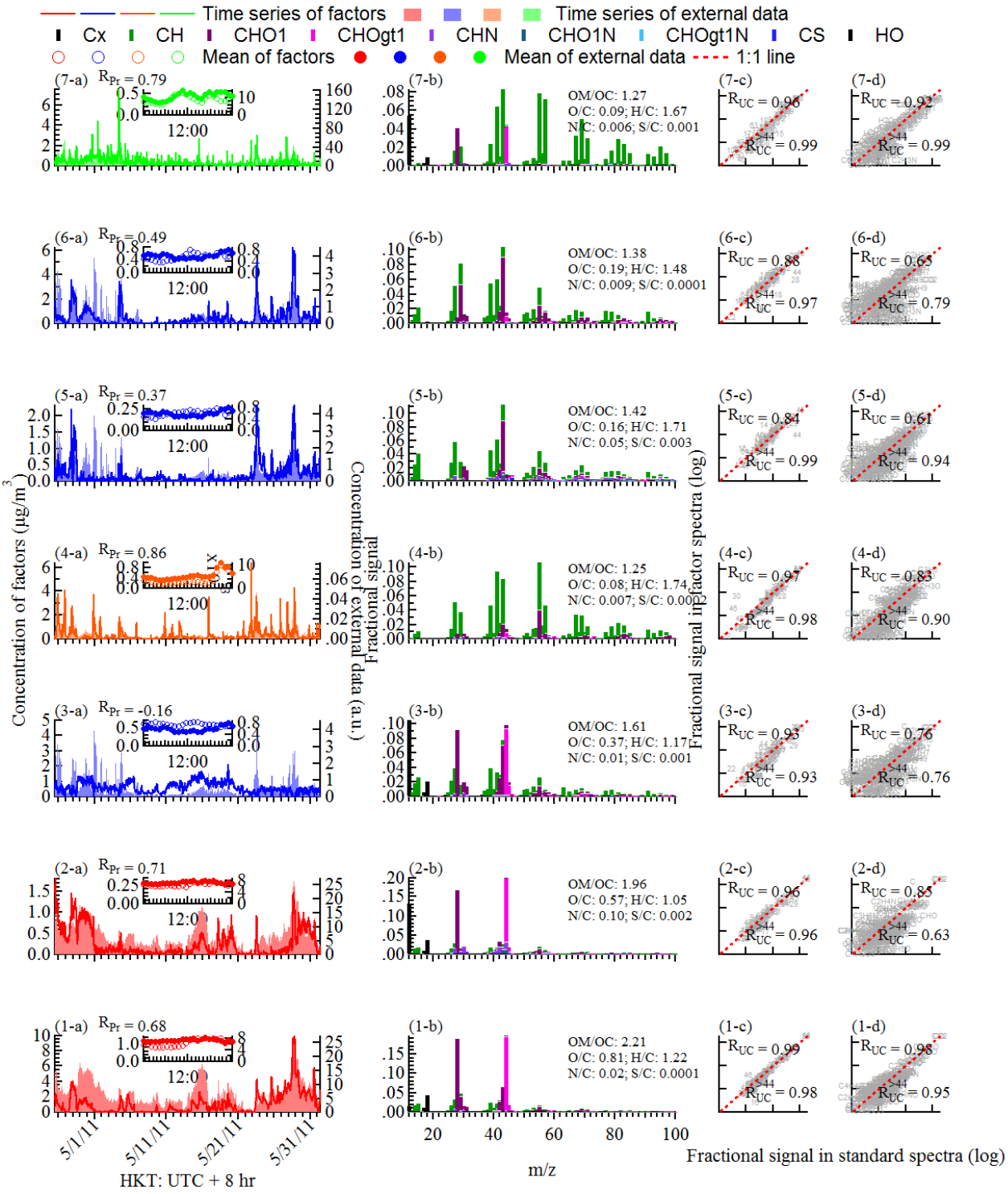

Figure S10 Original 7-factor solution for 201105, spring.

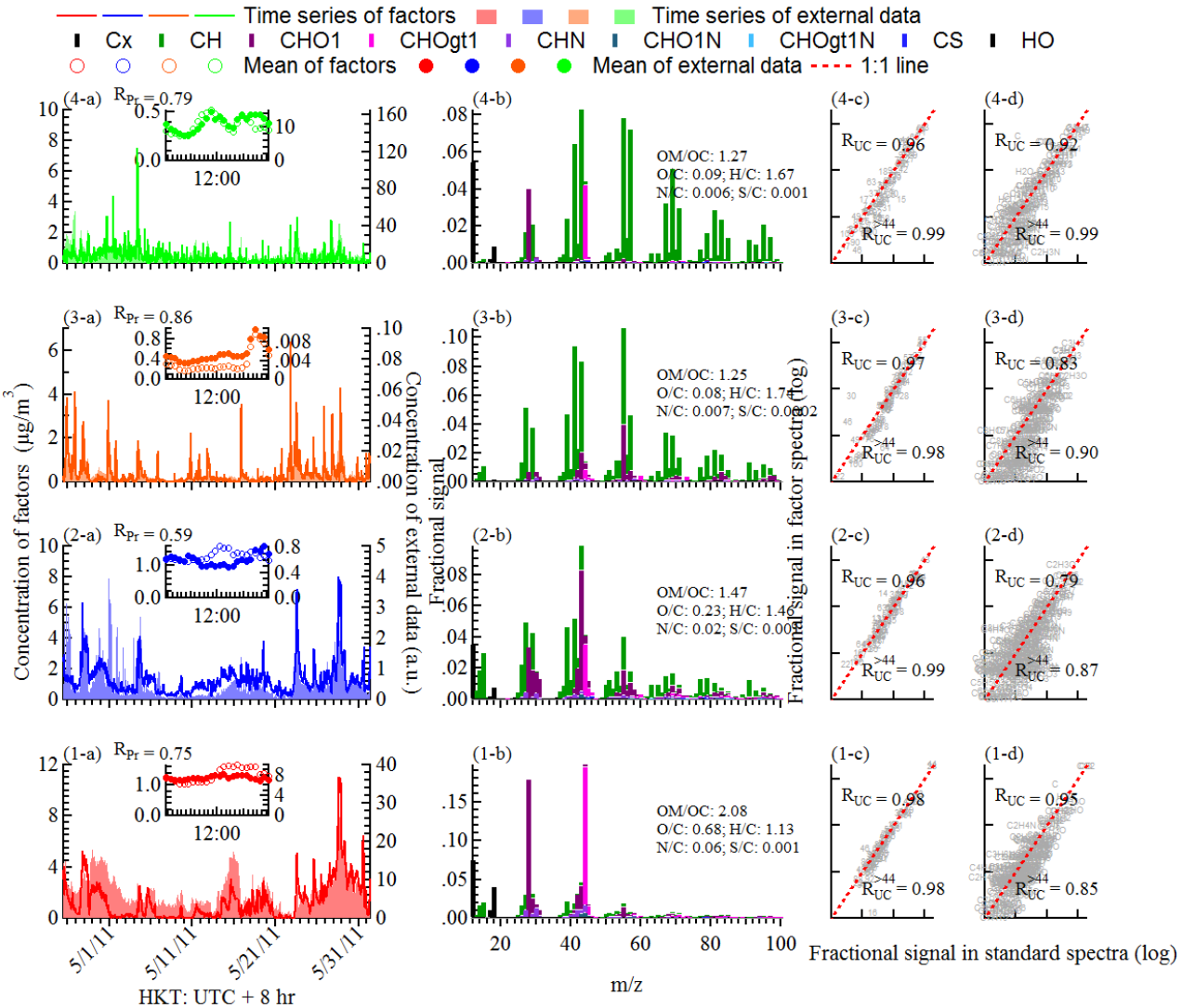

Figure S11 Combined 4-factor solution for 201105, spring.

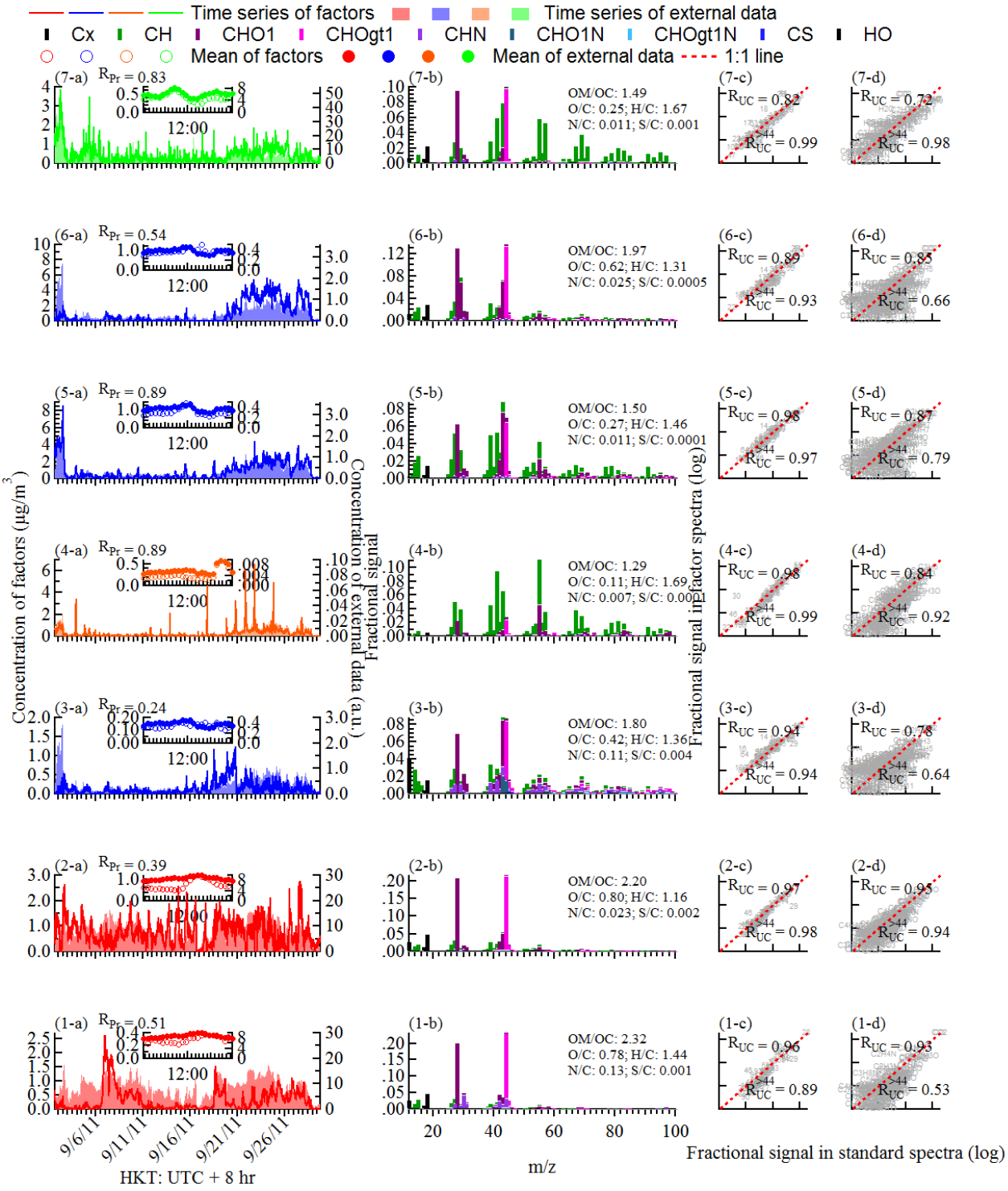

Figure S12 Original 7-factor solution for 201109, summer.

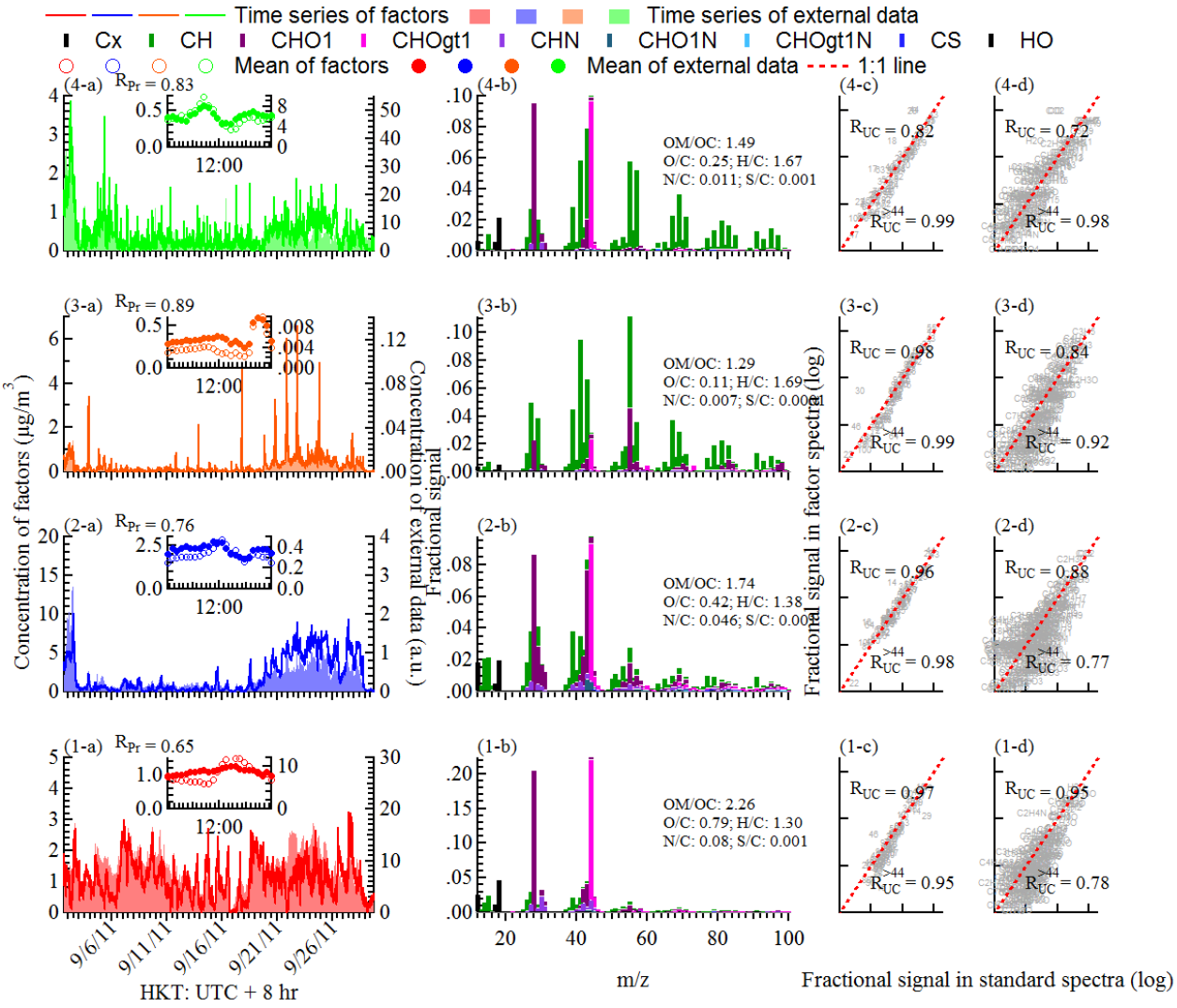

Figure S13 Combined 4-factor solution for 201109, summer.

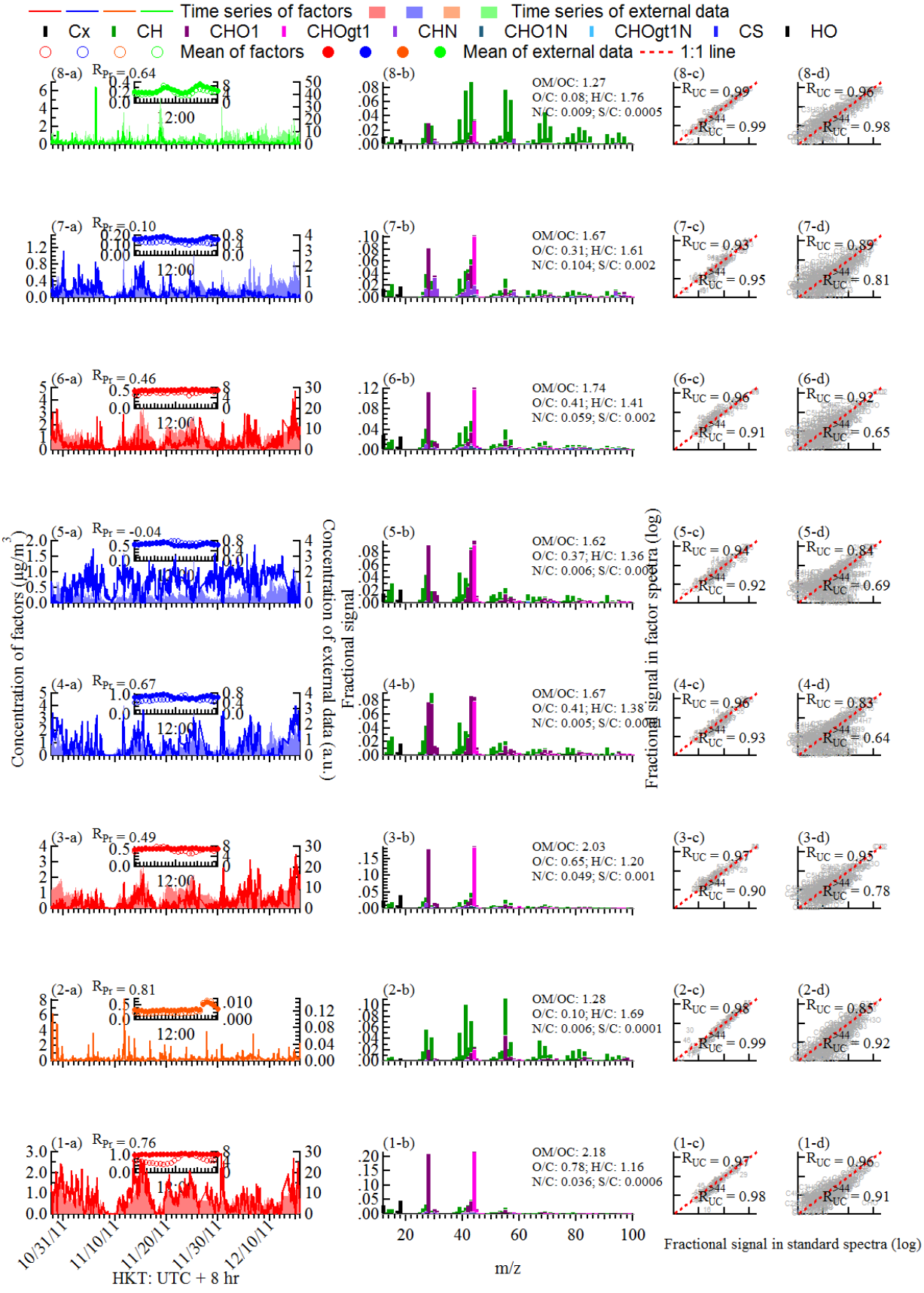

Figure S14 Original 8-factor solution for 201111, autumn.

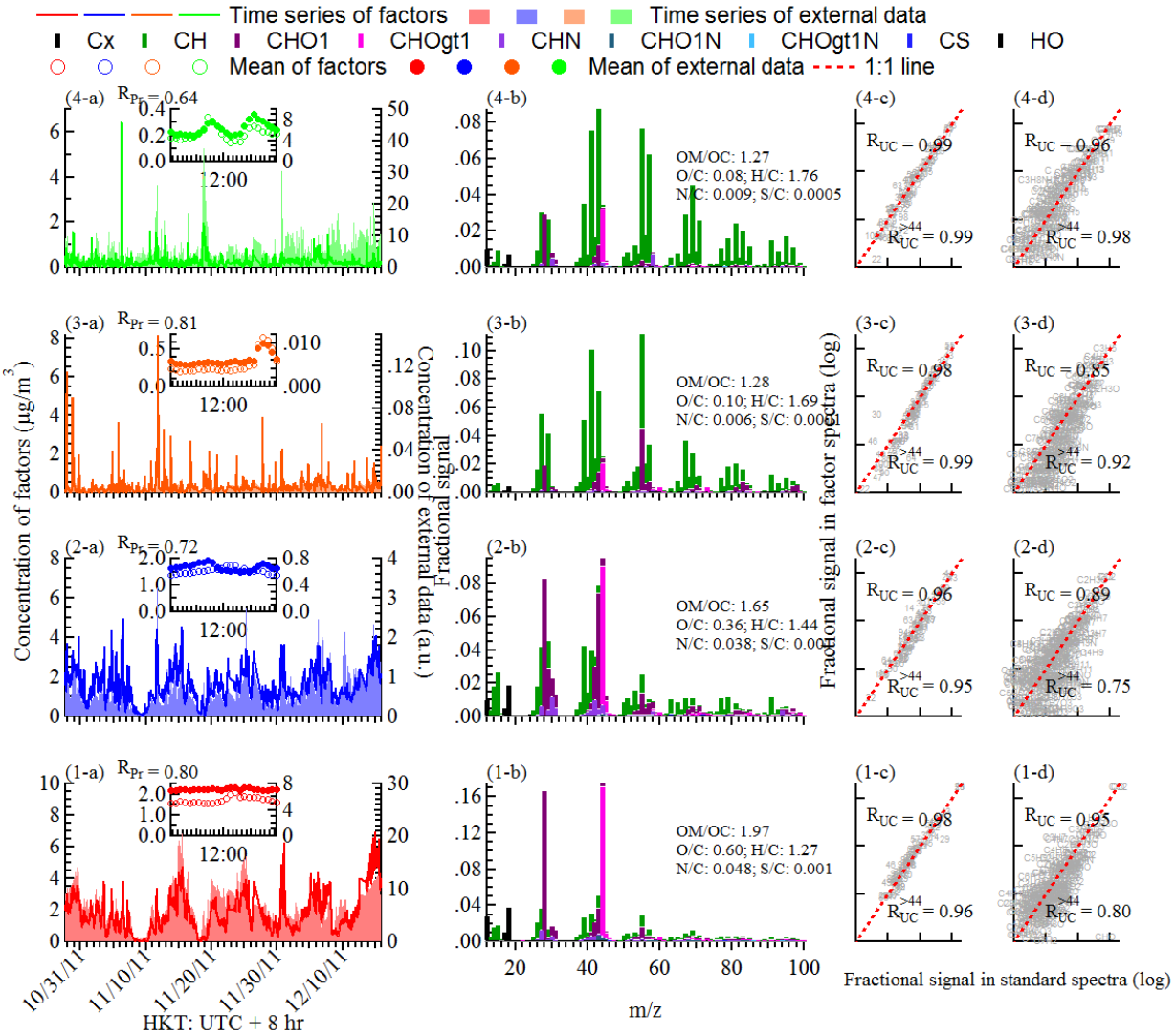

Figure S15 Combined 4-factor solution for 201111, autumn.

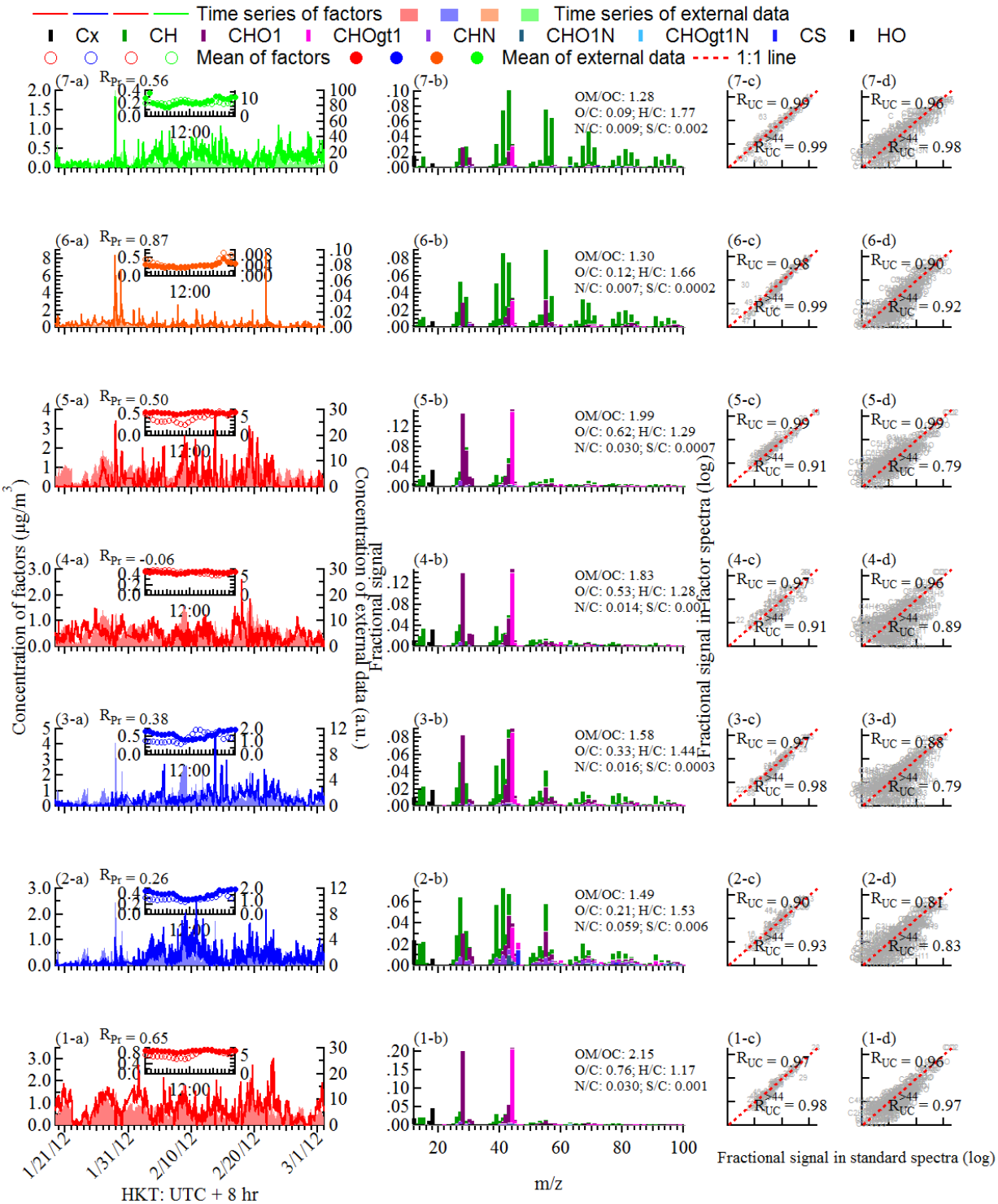

Figure S16 Original 7-factor solution for 201202, winter.

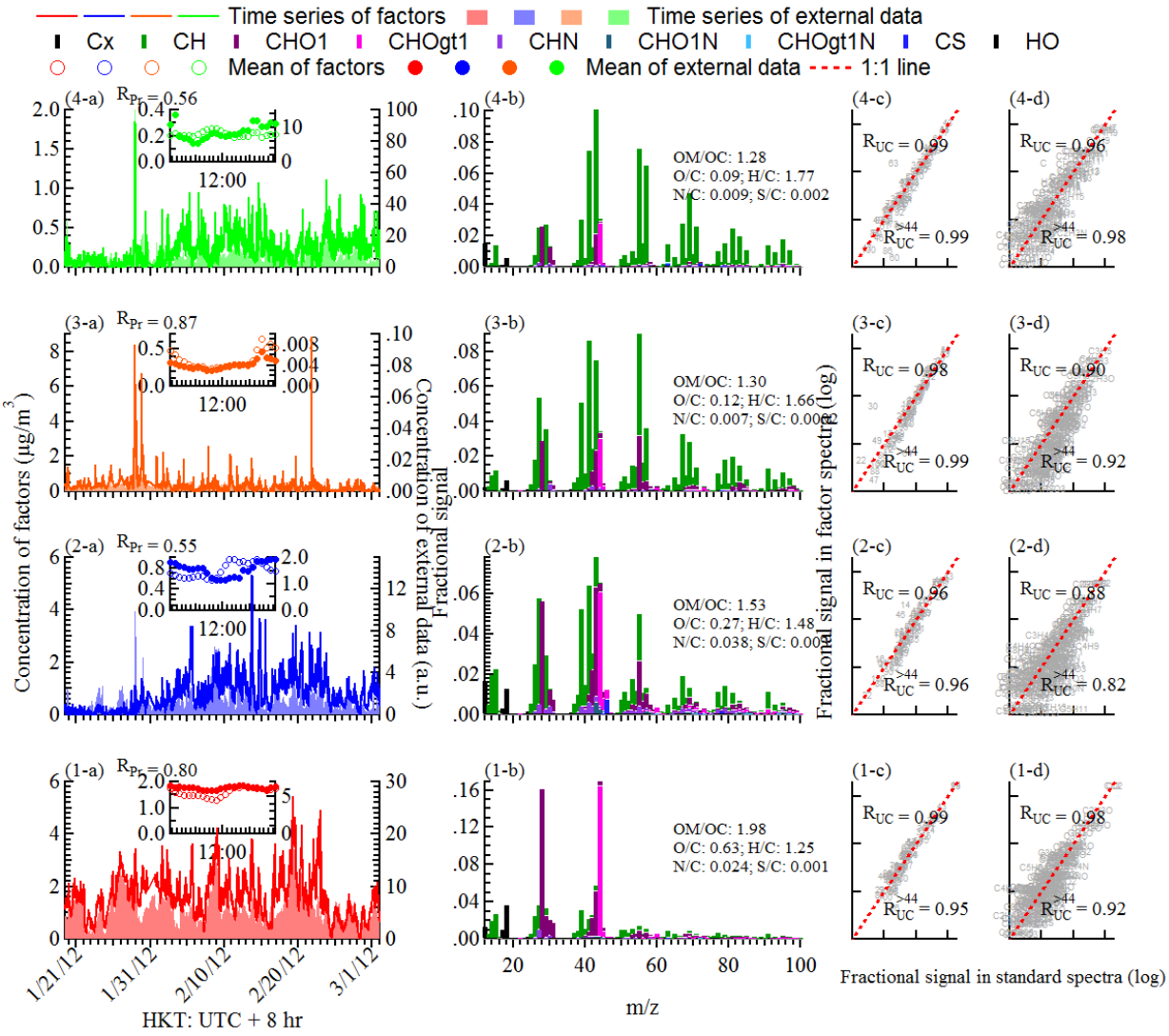

Figure S17 Combined 4-factor solution for 201202, winter.

Table S3 Summary of correlation coefficients of time series with external data and mass spectra with those in the literature. "3ions" means the three ions used as tracers for COA. R_{Pr} is the Pearson's R, R_{UC} is the un-centered R for whole mass spectra, and $R_{UV}^{>44}$ is the un-centered R for ions with m/z > 44.

Color code		R_{Pr}	<0.4	0.4< <0.6	0.6< <0.8	>0.8							Color code	R_{UC}	$R_{UC}^{>44}$	<0.7	0.7< <0.8	0.8< <0.9	>0.9
Season	Factor	TS	R_{Pr}	Factor	TS	R_{Pr}	Factor	MS	UMR		HR		Factor	MS	UMR		HR		
									R_{UC}	$R_{UC}^{>44}$	R_{UC}	$R_{UC}^{>44}$			R_{UC}	$R_{UC}^{>44}$	R_{UC}	$R_{UC}^{>44}$
Spring, 201105	F1	SO4	0.68	F1	SO4	0.75	F1	LVOOA	0.99	0.98	0.98	0.95	F1	LVOOA	0.98	0.98	0.95	0.85
	F2	SO4	0.71	F2	NO3	0.59	F2	LVOOA	0.96	0.96	0.85	0.63	F2	SVOOA	0.96	0.99	0.79	0.87
	F3	NO3	-0.16	F3	COA_3ions	0.86	F3	SVOOA	0.93	0.93	0.76	0.76	F3	COA	0.97	0.98	0.83	0.90
	F4	3ions	0.86	F4	NOx	0.79	F4	COA	0.97	0.98	0.83	0.90	F4	HOA	0.96	0.99	0.92	0.99
	F5	NO3	0.37				F5	SVOOA	0.84	0.99	0.61	0.94						
	F6	NO3	0.49				F6	SVOOA	0.88	0.97	0.65	0.79						
	F7	NOx	0.79				F7	HOA	0.96	0.99	0.92	0.99						
Summer, 201109	F1	SO4	0.51	F1	SO4	0.65	F1	LVOOA	0.96	0.89	0.93	0.53	F1	LVOOA	0.97	0.95	0.95	0.78
	F2	SO4	0.39	F2	NO3	0.76	F2	LVOOA	0.97	0.98	0.95	0.94	F2	SVOOA	0.96	0.98	0.88	0.77
	F3	NO3	0.24	F3	COA_3ions	0.89	F3	SVOOA	0.94	0.94	0.78	0.64	F3	COA	0.98	0.99	0.84	0.92
	F4	3ions	0.89	F4	NOx	0.83	F4	COA	0.98	0.99	0.84	0.92	F4	HOA	0.82	0.99	0.72	0.98
	F5	NO3	0.89				F5	SVOOA	0.98	0.97	0.87	0.79						
	F6	NO3	0.54				F6	SVOOA	0.89	0.93	0.85	0.66						
	F7	NOx	0.83				F7	HOA	0.82	0.99	0.72	0.98						
Autumn, 201111	F1	SO4	0.76	F1	SO4	0.80	F1	LVOOA	0.97	0.98	0.96	0.91	F1	LVOOA	0.98	0.96	0.95	0.80
	F2	3ions	0.81	F2	NO3	0.72	F2	COA	0.98	0.99	0.85	0.92	F2	SVOOA	0.96	0.95	0.89	0.75
	F3	SO4	0.49	F3	COA_3ions	0.81	F3	LVOOA	0.97	0.90	0.95	0.78	F3	COA	0.98	0.99	0.95	0.92
	F4	NO3	0.67	F4	NOx	0.64	F4	SVOOA	0.96	0.93	0.83	0.64	F4	HOA	0.99	0.99	0.96	0.98
	F5	NO3	-0.04				F5	SVOOA	0.94	0.92	0.84	0.69						
	F6	SO4	0.46				F6	LVOOA	0.96	0.91	0.92	0.65						
	F7	NO3	0.10				F7	SVOOA	0.93	0.95	0.89	0.81						
	F8	NOx	0.64				F8	HOA	0.99	0.99	0.96	0.98						
Winter, 201202	F1	SO4	0.65	F1	SO4	0.80	F1	LVOOA	0.97	0.98	0.96	0.97	F1	LVOOA	0.99	0.95	0.98	0.92
	F2	NO3	0.26	F2	NO3	0.55	F2	SVOOA	0.90	0.93	0.81	0.83	F2	SVOOA	0.96	0.96	0.88	0.82
	F3	NO3	0.38	F3	COA_3ions	0.87	F3	SVOOA	0.97	0.98	0.88	0.79	F3	COA	0.98	0.99	0.90	0.92
	F4	SO4	-0.06	F4	NOx	0.56	F4	LVOOA	0.97	0.91	0.96	0.89	F4	HOA	0.99	0.99	0.96	0.98
	F5	SO4	0.50				F5	LVOOA	0.99	0.91	0.99	0.79						
	F6	3ions	0.87				F6	COA	0.98	0.99	0.90	0.92						
	F7	NOx	0.56				F7	HOA	0.99	0.99	0.96	0.98						

Table S4 Elemental analysis for the four factors in four seasons.

	HOA				COA				SVOOA				LVOOA			
	OM/OC	O/C	H/C	N/C	OM/OC	O/C	H/C	N/C	OM/OC	O/C	H/C	N/C	OM/OC	O/C	H/C	N/C
Spr., 201105	1.27	0.09	1.67	0.01	1.25	0.08	1.74	0.01	1.47	0.23	1.46	0.02	2.08	0.68	1.13	0.06
Sum., 201109	1.49	0.25	1.67	0.01	1.29	0.11	1.69	0.01	1.74	0.42	1.38	0.05	2.26	0.79	1.30	0.08
Aut., 201111	1.27	0.08	1.76	0.01	1.28	0.10	1.69	0.01	1.65	0.36	1.44	0.04	1.97	0.60	1.27	0.05
Win., 201202	1.28	0.09	1.77	0.01	1.30	0.12	1.66	0.01	1.53	0.27	1.48	0.04	1.98	0.63	1.25	0.02

6. Back trajectory analysis evaluation

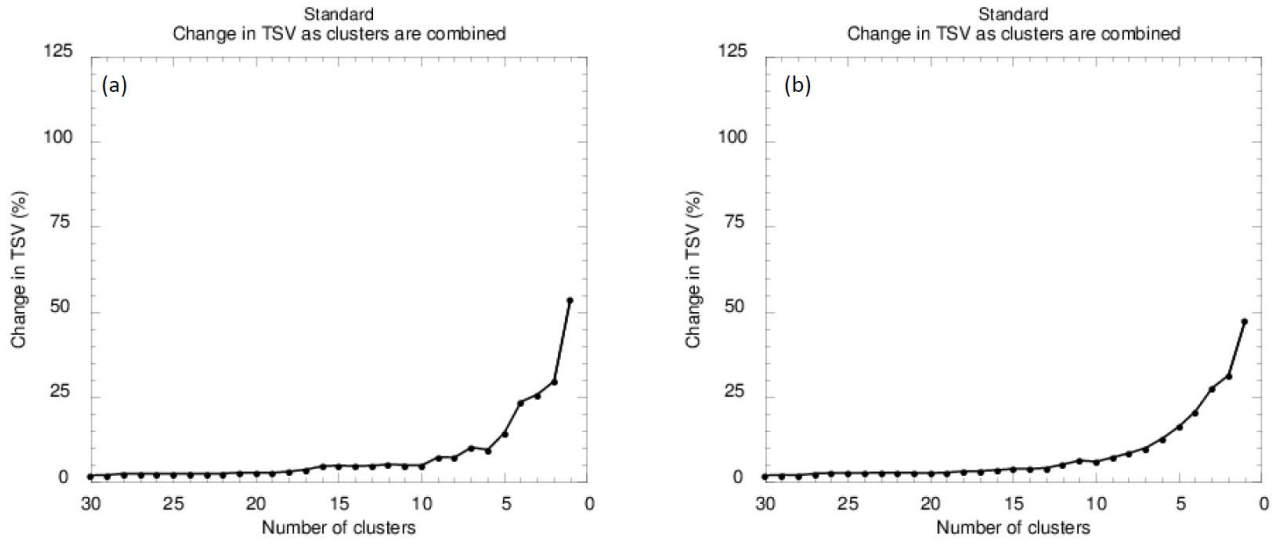

Figure S18 Total spatial variance (TSV) as a function of number of clusters for (a) 300 m and (b) arrival heights.

Figure S18 shows the changes in total spatial variance (TSV) as a function of number of clusters for 300 m arrival height (left) and for 500 m arrival height (right). For both case, the changes in TSV decreased substantially from 4 to 6 cluster solutions. Therefore, solutions (shown in Figure S19) with 4, 5, and 6 clusters for both arrival heights were obtained and subject to further evaluation.

Species concentrations of distinct sources as indicators of (a) transported species (sulfate and LVOOA) and (b) locally emitted species (HOA and COA) were used for the evaluation. The concentrations of these four species in each cluster are plotted in box-whisker plots as shown in Figures S20 and S21 for 300 m and 500 m arrival height, respectively. The evaluation rationale is as follows: (1) a larger number of clusters can potentially provide more detailed information and should be attempted; (2) too many clusters may be purely mathematical and make little physical sense, thus should be avoided if it is the case; (3) transported species (mainly anthropogenic) should be associated with long trajectories from the continent; (4) locally emitted species should be associated with short trajectories with calm wind. The optimal number of clusters balancing points (1) and (2) is chosen with an evaluation of points (3) and (4) for the same arrival height. A similar evaluation using points (3) and (4) is employed to choose a final solution from the optimal solutions at each arrival height.

As shown in Figure S19 (a) to (c), going from the 4-cluster solution to the 5-cluster solution splits Cluster 2 in the 4-cluster solution into Clusters 2 and 5 in the 5-cluster solution, while going from the 5-cluster solution to the 6-cluster solution splits Cluster 3 into Clusters 3 and 5 in the 6-cluster solution. In Figure S20, the split of Cluster 2 in the 4-cluster solution into Cluster 2 and 5 in the 5-cluster solution

leads to slightly higher SO4 and SVOOA in Cluster 5 than in Cluster 2 in the 5-cluster solution, while to substantially lower HOA and COA in Cluster 5 than in Cluster 2 in the 5-cluster solution. This observation suggests that a split of the otherwise lumped Cluster 2 in the 4-cluster solution can provide consistent interpretation of regional and local pollutants. One the other hand, from panels (b) to panels (c) in Figure S20, the split of Cluster 3 in the 5-cluster solution into Clusters 3 and 5 in the 6-cluster solution does not lead to such consistency. In the 6-cluster solution, SO4 in Cluster 3 is higher than in Cluster 5 (c-1), while LVOOA in Cluster 3 is lower than in Cluster 5 (c-2). Similarly, HOA in Cluster 3 is higher than in Cluster 5 (c-3), while COA in Cluster 3 is lower than in Cluster 5 (c-4). This observation suggests that going from 5-cluster solution to 6-cluster solution does not provide additional information that is consistent with the tracer species concentrations.

As shown in Figure S19 (d) to (f), going from the 4-cluster solution to the 5-cluster solution splits Cluster 1 in the 4-cluster solution into Clusters 1 and 2 in the 5-cluster solution, while going from the 5-cluster solution to the 6-cluster solution splits Cluster 2 into Clusters 2 and 3 in the 6-cluster solution. In Figure S21, the split of Cluster 1 in the 4-cluster solution to Clusters 1 and 2 in the 5-cluster solution leads to lower concentrations in Cluster 1 and higher concentrations in Cluster 2 for all four species, indicating consistency. On the other hand, the split of Cluster 2 in the 5-cluster solution to Clusters 2 and 3 does not lead to such a consistency. SO4 concentration in Cluster 2 is lower than in Cluster 3, while LVOOA in Cluster 2 is higher than in Cluster 3 in the 6-cluster solution. The effect is less pronounced for HOA but HOA in Cluster 2 is slightly higher than in Cluster 3, while COA in Cluster

2 is much higher than in Cluster 3 in the 6-cluster solution. Therefore, going from 5-cluster solution to 6-cluster solution does not provide consistent interpretation of the tracer species concentrations.

5-cluster solutions from both the arrival heights seems reasonable. The major difference between these two solutions is that the solution from arrival height of 300 m has a short trajectory (Cluster 3) representing the air mass circulating the Pearl River Delta (PRD) region (Figure S19-b, which cannot be captured by setting the arrival height of 500 m (Figure S19-e). Therefore, we choose the 5-cluster solution with arrival height of 300 m for the analysis to reflect the impact of the nearby PRD region.

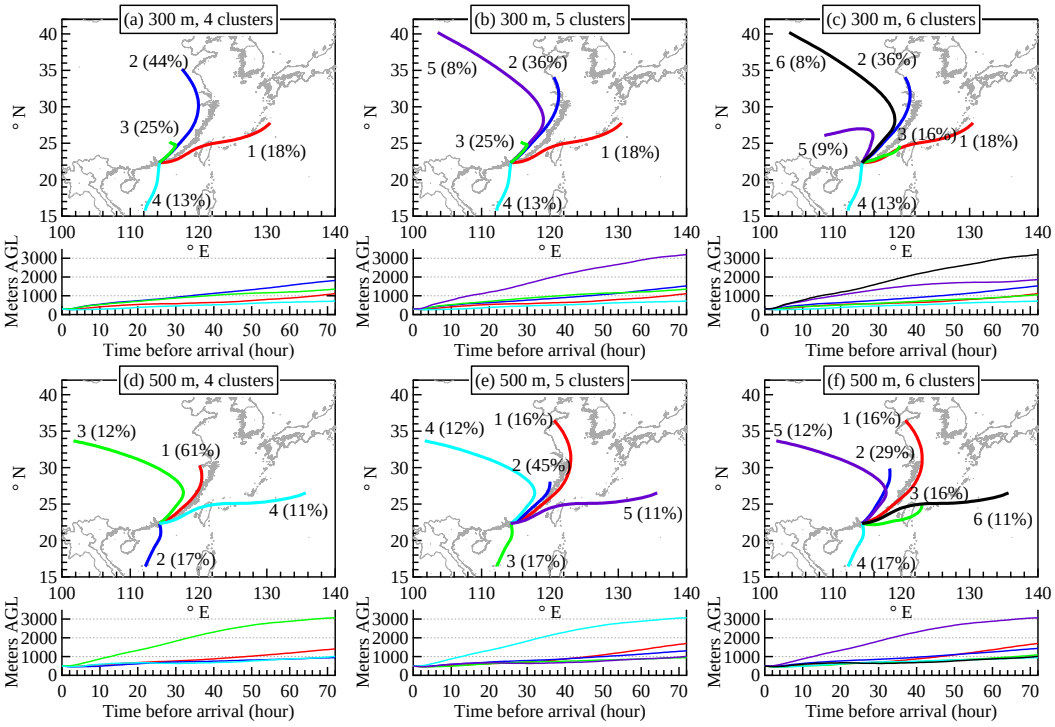

Figure S19 Solutions with 4 to 6 clusters for arrival height at 300 m (a – c) and 500 m (d – f).

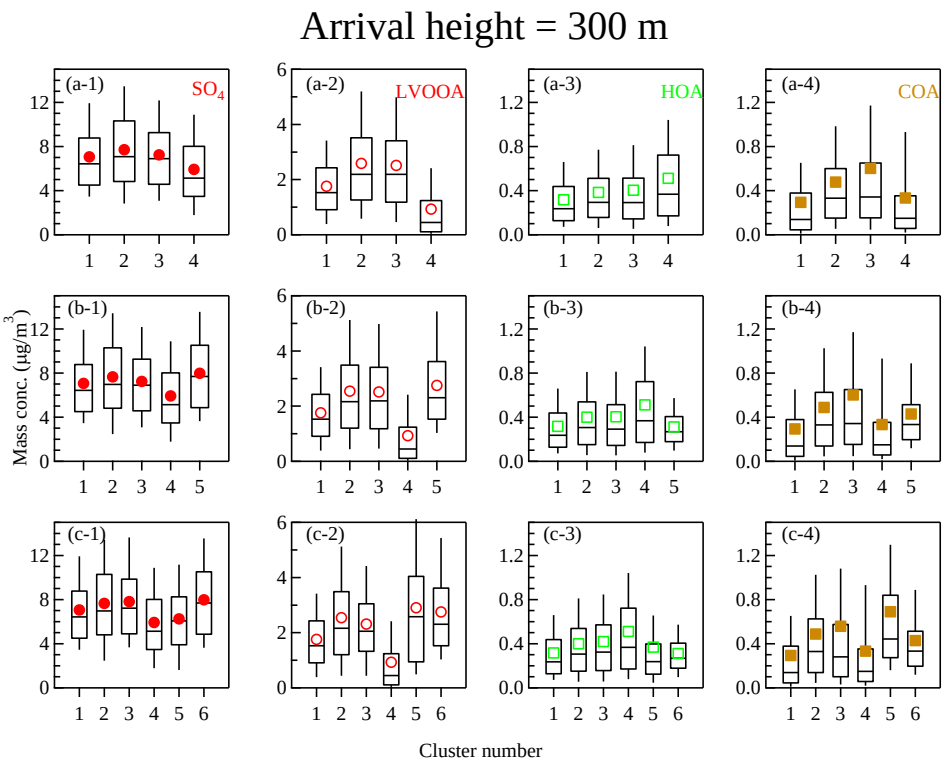

Figure S20 Mass concentrations of sulfate (a-1, b-1, and c-1), LVOOA (a-2, b-2, and c-2), HOA (a-3, b-3, and c-3), and COA (a-4, b-4, and c-4) for 4-cluster (panels a-1 to a-4), 5-cluster (panels b-1 to b-4), and 6-cluster (panels c-1 to c-4) solutions for arrival height at 300 m.

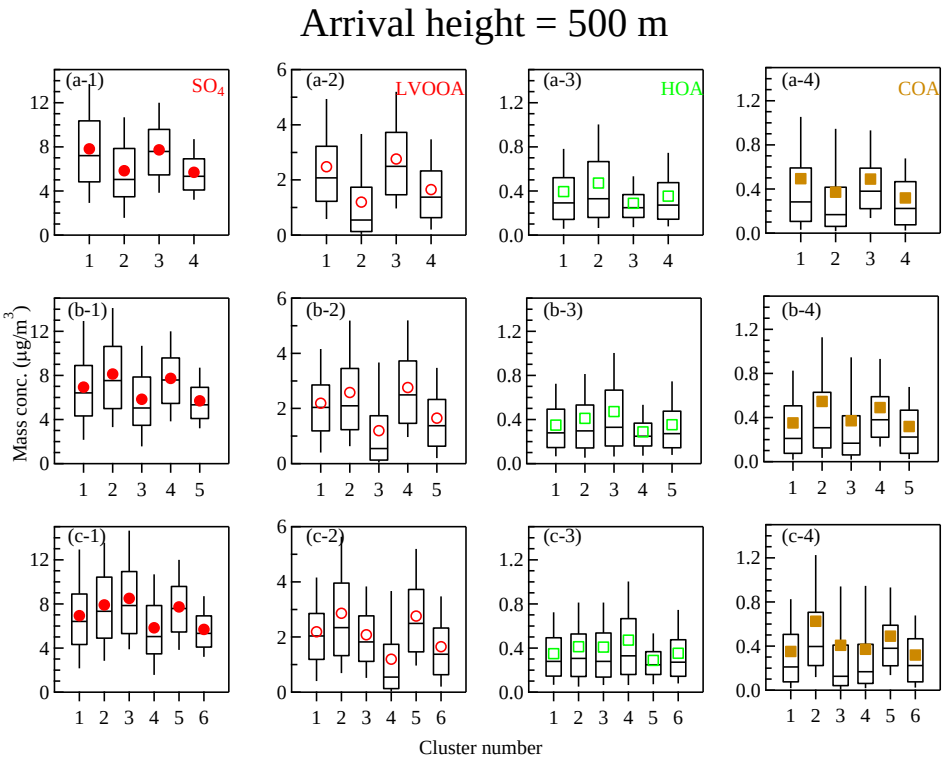

Figure S21 Mass concentrations of sulfate (a-1, b-1, and c-1), LVOOA (a-2, b-2, and c-2), HOA (a-3, b-3, and c-3), and COA (a-4, b-4, and c-4) for 4-cluster (panels a-1 to a-4), 5-cluster (panels b-1 to b-4), and 6-cluster (panels c-1 to c-4) solutions for arrival height at 500 m.

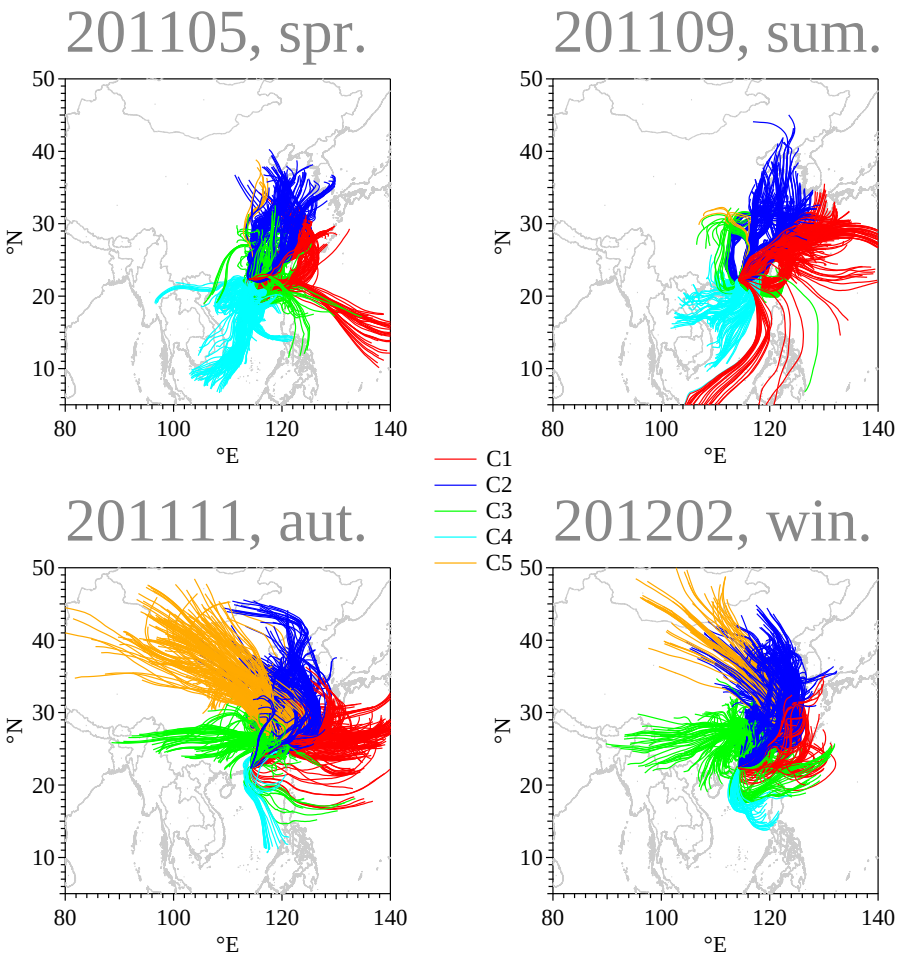

Figure S22 Individual trajectories in each measurement month colored coded by clusters.

7. Reference

Bahreini, R., Jimenez, J. L., Wang, J., Flagan, R. C., Seinfeld, J. H., Jayne, J. T., and Worsnop, D. R.: Aircraft-based aerosol size and composition measurements during ACE-Asia using an Aerodyne aerosol mass spectrometer, J. Geophys. Res.-Atmos., 108, 10.1029/2002jd003226, 2003.

Collier, S., and Zhang, Q.: Gas-Phase CO2 Subtraction for Improved Measurements of the Organic Aerosol Mass Concentration and Oxidation Degree by an Aerosol Mass Spectrometer, Environ. Sci. Technol., 47, 14324-14331, 2013.

DeCarlo, P. F., Slowik, J. G., Worsnop, D. R., Davidovits, P., and Jimenez, J. L.: Particle morphology and density characterization by combined mobility and aerodynamic diameter measurements. Part 1: Theory, Aerosol Sci. Technol., 38, 1185-1205, 2004.

Gong, Z. H., Lan, Z. J., Xue, L., Zeng, L. W., He, L. Y., and Huang, X. F.: Characterization of

submicron aerosols in the urban outflow of the central Pearl River Delta region of China, Front. Env. Sci. Eng., 6, 725-733, 2012.
Gunthe, S. S., Rose, D., Su, H., Garland, R. M., Achtert, P., Nowak, A., Wiedensohler, A., Kuwata, M., Takegawa, N., Kondo, Y., Hu, M., Shao, M., Zhu, T., Andreae, M. O., and Poschl, U.: Cloud condensation nuclei (CCN) from fresh and aged air pollution in the megacity region of Beijing, Atmos. Chem. Phys., 11, 11023-11039, 2011.
Han, Y. M., Iwamoto, Y., Nakayama, T., Kawamura, K., and Mochida, M.: Formation and evolution of biogenic secondary organic aerosol over a forest site in Japan, J. Geophys. Res.-Atmos., 119, 259-273, 2014.
He, L. Y., Huang, X. F., Xue, L., Hu, M., Lin, Y., Zheng, J., Zhang, R. Y., and Zhang, Y. H.: Submicron aerosol analysis and organic source apportionment in an urban atmosphere in Pearl River Delta of China using high-resolution aerosol mass spectrometry, J. Geophys. Res.-Atmos., 116, Artn D12304, Doi 12310.11029/12010jd014566, 2011.
Hu, W. W., Hu, M., Yuan, B., Jimenez, J. L., Tang, Q., Peng, J. F., Hu, W., Shao, M., Wang, M., Zeng, L. M., Wu, Y. S., Gong, Z. H., Huang, X. F., and He, L. Y.: Insights on organic aerosol aging and the influence of coal combustion at a regional receptor site of central eastern China, Atmos. Chem. Phys., 13, 10095-10112, 2013.
Huang, X. F., He, L. Y., Hu, M., Canagaratna, M. R., Sun, Y., Zhang, Q., Zhu, T., Xue, L., Zeng, L. W., Liu, X. G., Zhang, Y. H., Jayne, J. T., Ng, N. L., and Worsnop, D. R.: Highly time-resolved chemical characterization of atmospheric submicron particles during 2008 Beijing Olympic Games using an Aerodyne High-Resolution Aerosol Mass Spectrometer, Atmos. Chem. Phys., 10, 8933-8945, 2010.
Huang, X. F., He, L. Y., Hu, M., Canagaratna, M. R., Kroll, J. H., Ng, N. L., Zhang, Y. H., Lin, Y., Xue, L., Sun, T. L., Liu, X. G., Shao, M., Jayne, J. T., and Worsnop, D. R.: Characterization of submicron aerosols at a rural site in Pearl River Delta of China using an Aerodyne High-Resolution Aerosol Mass Spectrometer, Atmos. Chem. Phys., 11, 1865-1877, 2011.
Huang, X. F., He, L. Y., Xue, L., Sun, T. L., Zeng, L. W., Gong, Z. H., Hu, M., and Zhu, T.: Highly time-resolved chemical characterization of atmospheric fine particles during 2010 Shanghai World Expo, Atmos. Chem. Phys., 12, 4897-4907, 2012.
Huang, X. F., Xue, L., Tian, X. D., Shao, W. W., Sun, T. L., Gong, Z. H., Ju, W. W., Jiang, B., Hu, M., and He, L. Y.: Highly time-resolved carbonaceous aerosol characterization in Yangtze River Delta of China: Composition, mixing state and secondary formation, Atmos. Environ., 64, 200-207, 2013.
Park, K., Park, J., Lee, S., Cho, H. J., and Kang, M.: Real time measurement of chemical composition of submicrometer aerosols at urban Gwangju in Korea by aerosol mass spectrometer, Atmos. Environ., 62, 281-290, 2012.
Setyan, A., Zhang, Q., Merkel, M., Knighton, W. B., Sun, Y., Song, C., Shilling, J. E., Onasch, T. B., Herndon, S. C., Worsnop, D. R., Fast, J. D., Zaveri, R. A., Berg, L. K., Wiedensohler, A.,

Flowers, B. A., Dubey, M. K., and Subramanian, R.: Characterization of submicron particles influenced by mixed biogenic and anthropogenic emissions using high-resolution aerosol mass spectrometry: results from CARES, Atmos. Chem. Phys., 12, 8131-8156, 2012.

Sun, J. Y., Zhang, Q., Canagaratna, M. R., Zhang, Y. M., Ng, N. L., Sun, Y. L., Jayne, J. T., Zhang, X. C., Zhang, X. Y., and Worsnop, D. R.: Highly time- and size-resolved characterization of submicron aerosol particles in Beijing using an Aerodyne Aerosol Mass Spectrometer, Atmos. Environ., 44, 131-140, 2010.

Sun, Y. L., Wang, Z. F., Dong, H. B., Yang, T., Li, J., Pan, X. L., Chen, P., and Jayne, J. T.: Characterization of summer organic and inorganic aerosols in Beijing, China with an Aerosol Chemical Speciation Monitor, Atmos. Environ., 51, 250-259, 2012.

Sun, Y. L., Wang, Z. F., Fu, P. Q., Jiang, Q., Yang, T., Li, J., and Ge, X. L.: The impact of relative humidity on aerosol composition and evolution processes during wintertime in Beijing, China, Atmos. Environ., 77, 927-934, 2013.

Takami, A., Miyoshi, T., Shimono, A., and Hatakeyama, S.: Chemical composition of fine aerosol measured by AMS at Fukue Island, Japan during APEX period, Atmos. Environ., 39, 4913-4924, 2005.

Takami, A., Miyoshi, T., Shimono, A., Kaneyasu, N., Kato, S., Kajii, Y., and Hatakeyama, S.: Transport of anthropogenic aerosols from Asia and subsequent chemical transformation, J. Geophys. Res.-Atmos., 112, 2007.

Takegawa, N., Miyakawa, T., Kondo, Y., Jimenez, J. L., Zhang, Q., Worsnop, D. R., and Fukuda, M.: Seasonal and diurnal variations of submicron organic aerosol in Tokyo observed using the Aerodyne aerosol mass spectrometer, J. Geophys. Res.-Atmos., 111, 2006.

Topping, D., Coe, H., McFiggans, G., Burgess, R., Allan, J., Alfarra, M. R., Bower, K., Choularton, T. W., Decesari, S., and Facchini, M. C.: Aerosol chemical characteristics from sampling conducted on the Island of Jeju, Korea during ACE Asia, Atmos. Environ., 38, 2111-2123, 2004.

Xiao, R., Takegawa, N., Zheng, M., Kondo, Y., Miyazaki, Y., Miyakawa, T., Hu, M., Shao, M., Zeng, L., Gong, Y., Lu, K., Deng, Z., Zhao, Y., and Zhang, Y. H.: Characterization and source apportionment of submicron aerosol with aerosol mass spectrometer during the PRIDE-PRD 2006 campaign, Atmos. Chem. Phys., 11, 6911-6929, 2011.

Zhang, J. K., Sun, Y., Liu, Z. R., Ji, D. S., Hu, B., Liu, Q., and Wang, Y. S.: Characterization of submicron aerosols during a month of serious pollution in Beijing, 2013, Atmos. Chem. Phys., 14, 2887-2903, 2014.

Zhang, Q., Meng, J., Quan, J., Gao, Y., Zhao, D., Chen, P., and He, H.: Impact of aerosol composition on cloud condensation nuclei activity, Atmos. Chem. Phys., 12, 3783-3790, 2012.